Papers

Multicomponent affinity radial flow chromatography

Tingyue Gu

Department of Chemical Engineering, Ohio University, Athens, OH, USA

Gow-Jen Tsai

School of Chemical Engineering, Purdue University, West Lafayette, IN, USA

George T. Tsao

Laboratory of Renewable Resources Engineering, Purdue University, West Lafayette, IN, USA

Radial flow chromatography can provide high volumetric flow rates with small bed pressures. It is advantageous for use in affinity chromatography in which resolution requirements can be easily achieved because of highly selective biospecific binding. In this work a general multicomponent kinetic rate model has been formulated for the simulation of various aspects of radial flow affinity chromatography. The model accounts for radial dispersion, external mass transfer, intraparticle diffusion, second-order kinetics, and reactions between soluble ligands and the macromolecules in the elution stage of affinity chromatography. The model is solved with an efficient and robust numeric procedure that uses the finite element, the orthogonal collocation, and the Gear's stiff methods. Kinetic effects have been studied and compared with mass transfer effects. The three stages of affinity chromatography–frontal adsorption, wash, and elution–have been simulated. The effects of the concentration and the affinity of the soluble ligands used in the elution stage have been discussed.

Keywords: affinity; chromatography; radial; model

Introduction

Affinity chromatography has seen rapid growth in recent years. It is widely considered as the most powerful means of separating and purifying enzymes, antibodies, antigens, and many other proteins and macromolecules that are of important use in scientific research and development of novel pharmaceuticals.[1] Affinity chromatography not only purifies a product but also concentrates the product to a considerable extent. Over the years, this subject has been reviewed by many people, most recently by Chase[1] and Liapis.[2] Affinity chromatography is also referred to as biospecific adsorption, because it uses the biospecific binding between the solute molecules and the immobilized ligands. The monovalent binding between a ligand and a solute macromolecule is generally considered as having a second-order kinetics.

There are two kinds of bindings in affinity chromatography: specific and nonspecific. The specific binding usually involves only the target macromolecule and the ligand. Nonspecific binding is undesirable but often unavoidable. It can be caused by unintended ion-exchange effects, hydrophobic effects, and so on.[1] The operational stages of affinity chromatography often include adsorption, washing, and elution. The column is regenerated after each cycle. The adsorption stage is carried out in the form of frontal adsorption. The washing stage right after the adsorption stage is aimed at removing the impurities in the bulk fluid and in the stagnant fluid inside particles, and impurities bonded to the support via nonspecific binding.[1]

The elution stage removes the bonded target macromolecules from the ligands. Elution can be carried out

Address reprint requests to Dr. Tsao at the Laboratory of Renewable Resources Engineering, Purdue University, 1295 Potter Center, West Lafayette, IN 47907-1295, USA.
Received 18 July 1991; accepted 23 April 1992

by using a soluble ligand, which is often the same as that immobilized on the support, if the soluble ligand is present in a higher concentration and is relatively inexpensive. The other method is often called nonspecific desorption, which uses a variety of eluting agents, such as pH, protein denaturants, chaotropic agents, polarity reducing agents, and temperature[1] to destabilize the binding between the macromolecules and the ligands.

Elution in affinity chromatography carries a different meaning from that used in other forms of chromatography, such as adsorption and ion-exchange, in which elution means impulse analysis. To avoid confusion, impulse analysis in affinity chromatography is referred as zonal analysis.[3-5]

The Langmuir isotherm for biospecific binding, which comes from the second-order kinetics is characterized by a very large equilibrium constant and a very small saturation capacity, which indicates that the ligand density of an affinity matrix is often quite low. Because of the large equilibrium constant, the isotherm is often nonlinear even though the concentrations are often very low. A universal function has been developed by Lee et al.,[5] to measure the effects of isotherm nonlinearity in zonal analysis.

General rate models for axial flow chromatography have been developed by Arve and Liapis,[6,7] Lipais,[8] and Gu[9] for affinity chromatography. Their models consider various mass transfer mechanisms and a second-order kinetics between the immobilized ligands and the macromolecules, and between the soluble ligands and the macromolecules during elution. The model developed by Gu[9] also considers the size exclusion effect.

An attractive alternative to the conventional axial flow chromatography (AFC) for preparative and large-scale uses is the radial flow chromatography (RFC). The radial flow geometry provides a much larger flow area and thus permits a much higher volumetric flow rate. It was claimed that using RFC instead of AFC may improve productivity quite significantly.[10] The shorter

Notation

a_i constant in Langmuir isotherm for component i, $b_i C_i^{\infty}$
b_i adsorption equilibrium constant for component i, k_{ai}/k_{di}
Bi_i Biot number of mass transfer for component i, $k_i R_p/(\varepsilon_p D_{pi})$
$\overline{Bi}_i$ averaged Bi_i
C_{bi} bulk phase concentration of component i
C_{fi} feed concentration profile of component i, a time-dependent variable
C_{0i} concentration used for nondimensionalization, $\max\{C_{fi}(t)\}$
C_{pi} concentration of component i in the stagnant fluid phase inside particle macropores
C_{pi}^s concentration of component i in the solid phase of particle (mole adsorbate/unit volume of particle skeleton)
C_i^{∞} adsorption saturation capacity for component i (mole adsorbate/unit volume of particle skeleton)
c_{bi} C_{bi}/C_{0i}
c_{pi} C_{pi}/C_{0i}
c_{pi}^s C_{pi}^s/C_{0i}
c_i^{∞} C_i^{∞}/C_{0i}
D_{bi} axial or radial dispersion coefficient of component i
$\overline{D}_{bi}$ averaged D_{bi}
D_{pi} effective diffusivity of component i, porosity not included
Da_i^a Damkölher number for adsorption $V_b\varepsilon_b(k_{ai}C_{0i})/Q$
Da_i^d Damkölher number of desorption, $V_b\varepsilon_b k_{di}/Q$
h axial bed length of the radial flow column
k_i film mass transfer coefficient of component i
k_{ai} adsorption rate constant for component i
k_{di} desorption rate constant for component i
N number of interior collocation points
Ne number of quadratic elements
Ns number of components
Pe_i Peclet number of radial dispersion for component i, $v(X_1 - X_0)/D_{bi}$
Q volumetric flow rate of the mobile phase
R radial coordinate for particle
R_p particle radius
r $= R/R_p$
t time
v interstitial velocity
V_b bed volume for RFC column, $\pi h(X_1^2 - X_0^2)$
V_0 dimensionless constant, $\pi h X_0^2/V_b$ or $X_0^2/X_1^2 - X_0^2$
V dimensionless volumetric coordinate, $\pi h(X^2 - X_0^2)/V_b$ or $X^2 - X_0^2/X_1^2 - X_0^2 \in [0, 1]$
X radial coordinate for RFC column
X_1 outer radius of RFC column
X_0 inner radius of RFC column

Greek letters

α $= 2\sqrt{V + V_0}(\sqrt{1 + V_0} - \sqrt{V_0})$
ε_b bed void volume fraction
ε_p particle porosity
η_i dimensionless constant, $\varepsilon_p D_{pi}/R_p^2\ V_b\varepsilon_b/Q$
ξ_i dimensionless constant for component i, $3Bi_i\eta_i(1 - \varepsilon_b)/\varepsilon_b$
τ dimensionless time, $Qt/V_b\varepsilon_b$
τ_{imp} dimensionless time duration for a rectangular pulse of the sample
ϕ Lagrangian interpolation function

flow path of RFC compared with that of AFC often results in smaller retention times for RFC. Thus RFC may not be used for systems that require high resolutions while the sample solutes do not have sufficient retention. This shortcoming often does not exist in affinity chromatography in which the target macromolecule(s) is often strongly retained. The low bed pressure of RFC also helps reduce the bed compression if a soft affinity gel matrix is used.

RFC has been used for separations of various biologic products.[11-14] Rice[15] obtained approximate solutions for axial and radial flow absorbers. Recently, an accurate numeric treatment has been developed by Gu et al.[16] for the solution of a general rate model for multicomponent RFC. The model considers radial dispersion, external mass transfer, intraparticle diffusion, and nonlinear multicomponent isotherms. The radial dispersion and external mass transfer coefficients are treated as variables that are dependent on the changing linear flow velocity in the radial direction.

In this work, a general multicomponent rate model has been formulated for the study of radial flow affinity chromatography. The model considers radial dispersion, external mass transfer, intraparticle diffusion, second-order kinetics, and reaction between soluble ligands and the macromolecules in the elution stage of affinity chromatography. Kinetic effects have been studied and compared with mass transfer effects. Various other aspects of affinity chromatography have been discussed.

Mathematical model

A general multicomponent rate model for RFC consists of the two partial differential equations for each component, which are obtained from mass balances in the bulk fluid phase and particle phase, respectiively. The model system and numeric method was presented by Gu et al.[16] The model assumes local equilibrium between molecules in the fluid phase in the macropores of the particle and in the stationary phase. To account for the rate of binding kinetics the model needs to be extended as follows. The second-order kinetics assumes the following reversible binding and dissociation reaction:

$$P_i + L \underset{k_{di}}{\overset{k_{ai}}{\rightleftharpoons}} P_iL \tag{1}$$

where P_i is component i (macromolecule) and L represents the immobilized ligand. In this elementary reaction, the binding kinetics is of second order, and the dissociation first order, as shown in the following rate expression:

$$\frac{\partial C^s_{pi}}{\partial t} = k_{ai}C_{pi}\left(C^\infty - \sum_{j=1}^{Ns} C^s_{pj}\right) - k_{di}C^s_{pi} \tag{2}$$

where k_{ai} and k_{di} are the adsorption and desorption rate constants for component i, respectively. The rate constant k_{ai} has a unit of concentration over time, and the rate constant k_{di} has a unit of inverse time.

Introducing dimensionless groups $Da^a_i = V_b\varepsilon_b(k_{ai}C_{0i})/Q$ and $Da^d_i = V_b\varepsilon_b k_{di}/Q$, which are defined as the Damkölher numbers[18] for adsorption and desorption, respectively, Equation 2 can be nondimensionalized as follows:

$$\frac{\partial c^s_{pi}}{\partial \tau} = Da^a_i c_{pi}\left(c^\infty - \sum_{j=1}^{Ns}\frac{C_{0j}}{C_{0i}}c^s_{pj}\right) - Da^d_i c^s_{pi} \tag{3}$$

The Damkölher numbers reflect the characteristic reaction times over that of the stoichiometric time. If the adsorption and desorption rates are sufficiently high compared with mass transfer rates an equilibrium can be assumed for each component between the stagnant fluid phase and the solid phase of the particles. By setting the left-hand side of Equation 3 to zero, the following Langmuir isotherm can be obtained:

$$C^s_{pi} = \frac{a_iC_{pi}}{1 + \sum_{j=1}^{Ns} b_jC_{pj}}, \text{ i.e.,}$$

$$c^s_{pi} = \frac{a_ic_{pi}}{1 + \sum_{j=1}^{Ns}(b_jC_{0j})c_{pj}} \text{ (dimensionless)} \tag{4}$$

where $a_i = C^\infty b_i$, $b_iC_{0i} = Da^a_i/Da^d_i$ and $a_i = C^\infty b_i = c^\infty Da^a_i/Da^d_i$. The adsorption saturation capacities for all the components in a multicomponent system are the same in this work. The $b_i = k_{ai}/k_{di}$ values for affinity chromatography are often very large,[19] but it is erroneous to jump to the conclusion depending on this alone that the desorption rate must be much smaller than that of adsorption, because the two processes have different reaction orders, and the concentration C_{pi} is often very small at the adsorption side of Equation 2. It should be pointed out that the multicomponent Langmuir isotherm is thermodynamically inconsistent if the saturation capacities of all the components are not the same.[20] Recently, Gu et al.[17] proposed a new isotherm for cer-

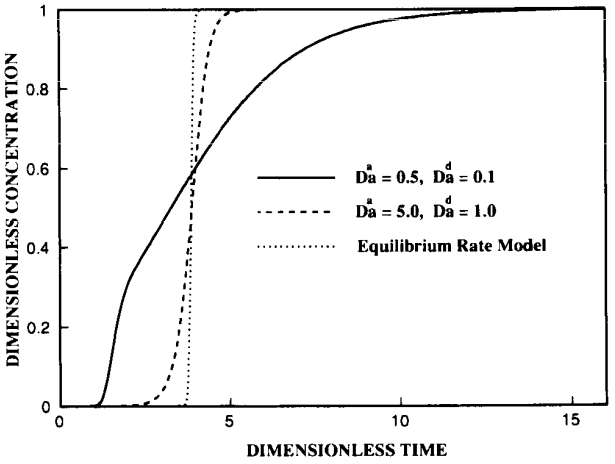

Figure 1 Effect of reaction rates in frontal analysis.

Table 1 Parameter values* used for simulation

Figure	Species	Physical Parameters							Numeric Parameters	
		Pe_{Li}	η_i	Bi_i	c^*	C_{0i}/C_{01}	Da_i^a	Da_i^d	Ne	N
1	1	100	5	20	3		0.5	0.1	6	2
2	1	100	5	20	3		5	1	7	2
3	1	100	3	20	1		1	0.2	12	2
4	1	100	3	20	1		0.5	0.1	6	2
5	1	100	1	40	10		10	1	6	2
	1	100	1	40	10	1	10	1		
6	2	100	1	40		1	10	1	6	2
	3	100	1	40		1				
	1	100	1	40	10	1	10	1		
7	2	100	1	40		2	20	1	6	2
	3	100	1	40		1				
	1	100	1	40	10	1	10	1		
8	2	100	1	40		1	40	1	6	2
	3	100	1	40		1				

* Parameters values are for solid-line curves in figures. In all cases, $\varepsilon_b = \varepsilon_p = 0.4$. The sample size for *Figure 3* is $\tau_{imp} = 0.5$. All cases use inward flow. The error tolerance of the ODE solver is tol = 10^{-5}. Double precision is used in the Fortran code. CPU times on SUN 4/390 computer are *Figure 1* (solid line), 16.0 s; *Figure 3* (solid line), 2.54 min; *Figure 6*, 10.56 min; *Figure 7*, 10.33 min.

tain multicomponent systems with uneven saturation capacities.

The model system contains Equations 9 and 10 in Gu et al.,[16] and Equation 2 in this work. This spatial discretizations of the model equations are the same as described in Gu et al.[16] Equation 2 is already an ODE and thus needs no spatial discretization. If Ne elements and N interior collocation points are used for the discretizations of the bulk fluid phase equation and the particle phase equation, there will be Ns(2Ne + 1) (2N + 1) ODEs in the final ODEs system.

Results and discussion

Effect of reaction kinetics

Figure 1 shows the effect of reaction rates on frontal adsorption. Parameter values used for the simulation are listed in *Table 1*. The solid curve shows that when the Damkölher numbers for binding and dissociation are low the breakthrough curve takes off sharply at an earlier time and levels off later on quite slowly compared with other cases in the figure that have higher reaction rates. This indicates that when the reaction rates are slow while the mass transfer rates are not, many solute molecules do not have chances to adsorb onto the solid phase, and those that do are released slowly. Note that the dimensionless Damkölher numbers for adsorption and dissociation are proportional to binding and dissociation rate constants. The unit dimensionless time (τ = 1) is the column dead time at which the breakthrough curve of a nonadsorbing and diffusing component takes off from zero concentration to the unit dimensionless concentration.

Figure 2 shows that when the reaction rates increase to some extent the breakthrough curves will be very close to that of the equilibrium case. In fact the equilibrium case is the asymptotic limit of the breakthrough curves calculated from the kinetic rate model.

Figure 3 shows the effect of reaction rates in a single-component zonal elution case. The solid line shows that the elution peak appears early with a very sharp front. However, it has a very long tailing. This indicates that when the reaction rates are very low, a large portion of the solute molecules do not have a chance to bind with the ligands, and they are eluted out quite quickly. Conversely, those molecules that do bind with the ligands are dissociated very slowly, causing a long tail. This is partially reflected by the breakthrough curve shown as the solid line in Figure 1 because the two operational modes are interrelated. Figure 3 also shows that the peak front appears later, and the peak height reduces when the reaction rates increase. When

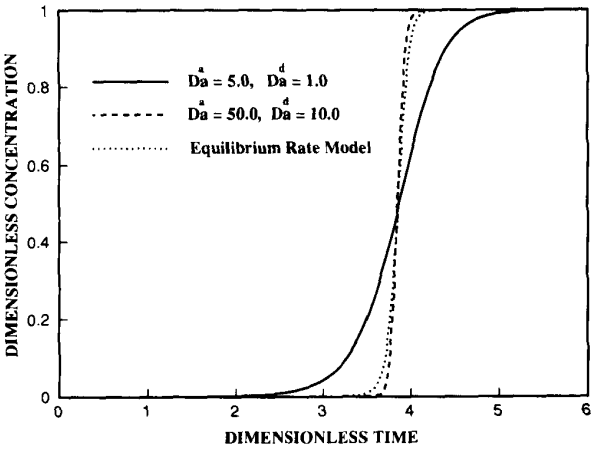

Figure 2 Fast reaction rates vs. equilibrium.

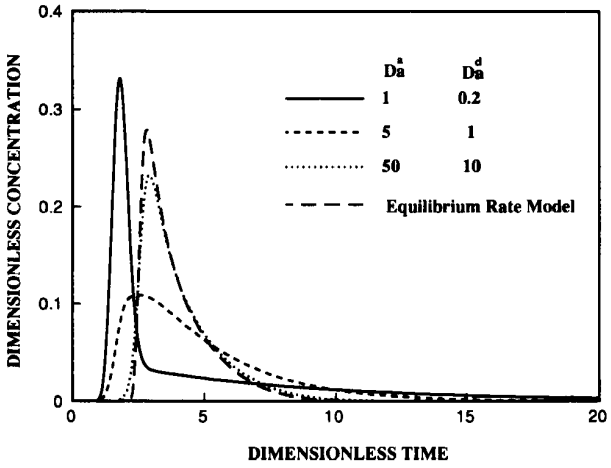

Figure 3 Effect of reaction rates in zonal analysis.

the reaction rates further increase the appearance of the peak front is further delayed, and the peak height increases, because the diffusion of the peak front owing to slow reaction rates is reduced. The increase of reaction rates clearly reduces the tailing effect as shown in Figure 3.

A breakthrough curve of an adsorption system with slow mass transfer rates is similar to that of slow reaction rates. They both take off sharply at an initial breakthrough time and level off later slowly. In Figure 4, one may find that the two cases differ in a revealing way. For the slow mass transfer case (dashed line), the breakthrough curve takes off earlier (at $\tau < 1$) than in the case with slow reaction rates (solid line), because in the former case, many solute molecules do not even enter the particles, whereas in the latter case they do.

Interaction between soluble ligand and macromolecule

Soluble ligands are often used to elute the adsorbed macromolecules in the elution stage, if the ligands are not expensive and can be easily separated from the macromolecules after elution.[1] A rate model involving soluble ligand used for the elution of a single adsorbate has been reported by Arve and Liapis[6,21] for finite baths and fixed beds with axial flow.

Modeling of reaction in fluid phase

The kinetic rate model described earlier in this work can be modified to include a binding reaction in the bulk fluid and the stagnant fluid in the particles between macromolecule P (component 1) and soluble ligand I (component 2). The complex formed from the binding of P and I is PI (component 3).

$$P + I \underset{k_{d2}}{\overset{k_{a2}}{\rightleftharpoons}} PI \tag{5}$$

The binding between the macromolecule and the immobilized ligand L forms PL.

$$P + L \underset{k_{d1}}{\overset{k_{a1}}{\rightleftharpoons}} PL \tag{6}$$

It is assumed that each macromolecule can bind with only one ligand, I or L, and there is no interaction between the two different ligands, I and L.

The following is a bulk fluid phase–governing equation:

$$-\frac{1}{X}\frac{\partial}{\partial X}\left(D_{bi}X\frac{\partial C_{bi}}{\partial X}\right) \pm v\frac{\partial C_{bi}}{\partial X} + \frac{\partial C_{bi}}{\partial t} + \frac{3k_i(1-\varepsilon_b)}{\varepsilon_b R_p}(C_{bi} - C_{pi,R=R_p}) - f(i)(k_{a2}C_{b1}C_{b2} - k_{d2}C_{b3}) = 0 \tag{7}$$

where $f(i) = -1$ for components 1 and 2 ($i = 1, 2$), and $f(i) = 1$ for component 3 ($i = 3$).

The following are particle phase–governing equations:

$$g(i)(1-\varepsilon_p)\frac{\partial C^s_{pi}}{\partial t} + \varepsilon_p\frac{\partial C_{pi}}{\partial t} - \varepsilon_p D_{pi}\left[\frac{1}{R^2}\frac{\partial}{\partial R}\left(R^2\frac{\partial C_{pi}}{\partial R}\right)\right] - f(i)\varepsilon_p(k_{a2}C_{p1}C_{p2} - k_{d2}C_{p3}) = 0 \tag{8}$$

$$\frac{\partial C^s_{p1}}{\partial t} = k_{a1}C_{p1}(C^\infty_1 - C^s_{p1}) - k_{d1}C^s_{p1} \tag{9}$$

in which $g(i) = 1$ for $i = 1$, and $g(i) = 0$ for $i = 2, 3$, because only component 1 binds with the immobilized ligand. The use of sign changers, $f(i)$ and $g(i)$, is purely for the compactness of the model system in its written form. Note that C^s_{p1} represents the concentration of the macromolecule in the solid phase (i.e., PL) based on the unit volume of the particle skeleton.

The model system is quite general because the size exclusion effect is included. It is actually more like that for a fixed-bed reactor than for chromatography,

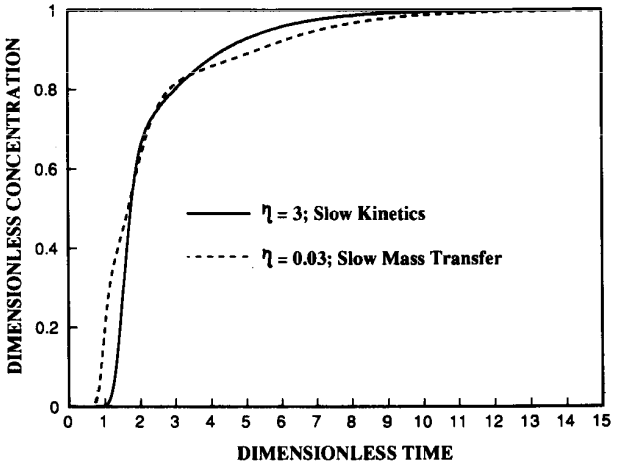

Figure 4 Comparison of slow kinetics with slow mass transfer.

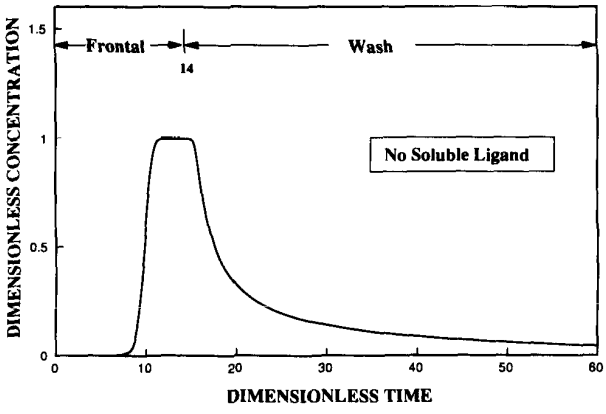

Figure 5 Frontal adsorption stage combined with wash stage.

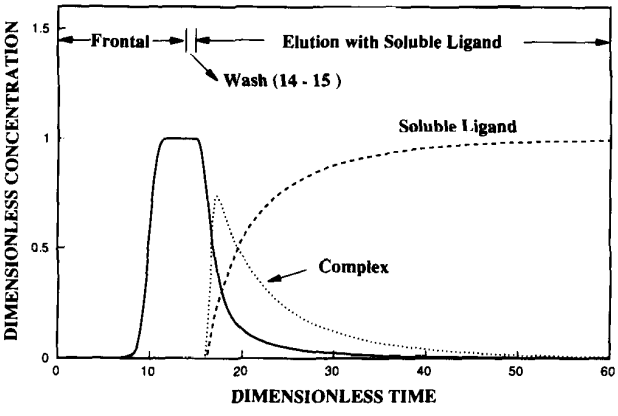

Figure 6 Effect of soluble ligand in elution.

because there is a new component (*PI*) forming and leaving the column.

Equations 7–9 can be expressed in the dimensionless form as follows:

$$-\frac{\partial}{\partial V}\left(\frac{\alpha}{Pe_i}\frac{\partial c_{bi}}{\partial V}\right) \pm \frac{\partial c_{bi}}{\partial V} + \frac{\partial c_{bi}}{\partial \tau} + \zeta_i(c_{bi} - c_{pi,r=1})$$

$$- f(i)\left(Da_2^a c_{b1}\frac{C_{02}}{C_{0i}}c_{b2} - Da_2^d\frac{C_{03}}{C_{0i}}c_{b3}\right) = 0 \quad (10)$$

$$g(i)\frac{\partial}{\partial \tau}(1-\varepsilon_p)c_{pi}^s + \varepsilon_p\frac{\partial c_{pi}}{\partial \tau}$$

$$- f(i)\varepsilon_p\left(Da_2^a c_{p1}\frac{C_{02}}{C_{0i}}c_{p2} - Da_2^d\frac{C_{03}}{C_{0i}}c_{p3}\right)$$

$$- \eta_i\left[\frac{1}{r^2}\frac{\partial}{\partial r}\left(r^2\frac{\partial c_{pi}}{\partial r}\right)\right] = 0 \quad (11)$$

$$\frac{\partial c_{p1}^s}{\partial \tau} = Da_1^a c_{p1}(c_1^\infty - c_{p1}^s) - Da_1^d c_{p1}^s \quad (12)$$

Because C_{03} is not known before simulation, it is replaced by C_{01} for the nondimensionalization of the concentrations of component 3 such that $C_{b3} = c_{b3}C_{01}$ and $C_{p3} = c_{p3}C_{01}$.

The model can be easily solved using the previous numerical procedure with modifications to include the reactions between the soluble ligands and macromolecules. Details have been reported by Gu.[9]

Modeling of three stages in affinity chromatography

Figure 5 shows an affinity chromatographic process with a wash stage after the frontal adsorption stage. The nonspecifically bound impurities are not included in the simulation. Their effluent histories can be simulated in a separate run and then superimposed onto the current figure, because they do not interact with the macromolecule. Because no soluble ligand or other active eluting agent is used for the elution, the chromatogram shows a very long tail, which indicates that the recovery of the macromolecule is difficult and not efficient for this sytem.

Figure 6 has the same condition as *Figure 5*, except that soluble ligands are used for elution at $\tau = 15$ after the wash stage which started at $\tau = 14$. Compared with

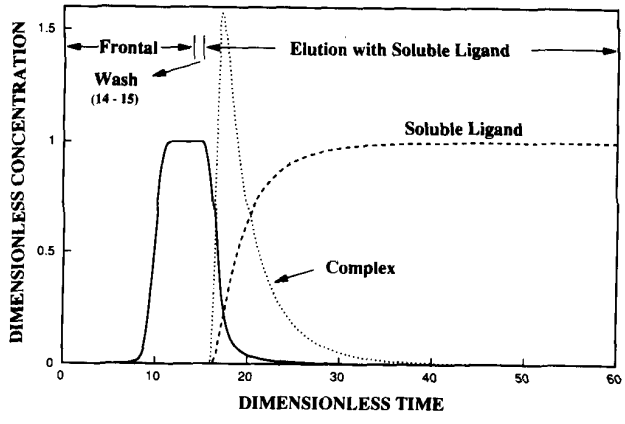

Figure 7 Effect of soluble ligand concentration in elution.

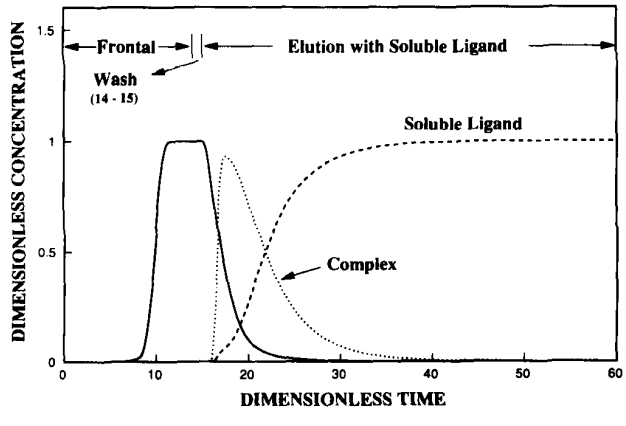

Figure 8 Effect of soluble ligand affinity with macromolecule in elution.

Figure 5, it is clear that elution using soluble ligands helps reduce tailing and the time needed for the recovery of the product. If a higher concentration of soluble ligand is used for elution, the elution stage will be shorter, and the recovered product can have a higher concentration as *Figure 7* shows, in which the soluble ligand concentration in the feed is twice of that in *Figure 6*.

Figure 8 has the same conditions as *Figure 6*, except that the reaction rate constant for the binding of the soluble ligand and the macromolecule, k_{a2}, is four times higher in *Figure 8* than in *Figure 6*. The comparison of the two figures shows that a higher k_{a2} value helps increase the efficiency of elution. It is also obvious that a higher k_{a2} value on the improvement of elution performance is not as effective as increasing the concentration of the soluble ligand as indicated by *Figure 7*.

Conclusion

In this article, a general multicomponent kinetic rate model has been formulated for the study of radial flow affinity chromatography. The model considers radial dispersion, external mass transfer, intraparticle diffusion and second-order kinetics. The model has also been modified to account for the reactions between macromolecules and soluble ligands in the bulk fluid and in the stagnant fluid inside particle macropores. Some important aspects of radial flow affinity chromatography, including the effects of reaction rates and mass transfer, have been discussed. The role of soluble ligand in the elution stage has been investigated.

Acknowledgments

We acknowledge financial support from National Science Foundation Grant EET-8613167A2.

References

1. Chase, H.A., Affinity separations utilizing immobilized monoclonal antibodies—a new tool for the biochemical engineer. *Chem. Eng. Sci.* 1984, **39,** 1099
2. Liapis, A.I. Theoretical aspects of affinity chromatography. *J. Biotech.* 1989, **11,** 143
3. Arnold, F.H., Schofield, S.A. and Blanch, H.W. Analytical affinity chromatography: I. Local equilibrium theory and the measurement of association and inhibition constants. *J. Chromatogr.* 1986, **355,** 1
4. Lee, W.-C. Radial flow chromatography with applications to bioseparation. Ph.D. diss., 1989. Purdue University, West Lafayette, IN, USA
5. Lee, W.-C., Tsai, G.-J. and Tsao, G.T. Radial-flow affinity chromatography for trypsin purification. *ACS Symp. Series* 1990, **427,** 104
6. Arve, B.H. and Liapis, A.I. Modeling and analysis of elution stage of biospecific adsorption in fixed beds. *Biotech. Bioeng.* 1987, **30,** 638
7. Arve, B.H. and Liapis, A.I. Biospecific adsorption in fixed and periodic countercurrent beds. *Biotech. Bioeng.* 1988, **32,** 616
8. Liapis, A.I., Modeling affinity chromatography. *Sep. Purif. Meth.* 1990, **19,** 133
9. Gu, T., Ph.D. diss., 1990. Purdue University, West Lafayette, IN, USA
10. McCormick, D. Chromatograph and affinity separations. *Bio/Technology* 1988, **6,** 158
11. Saxena, V., Weil, A.E., Kawahata, R.T., McGregor, W.C. and Chandler, M. Applications of radial flow columns for fast affinity chromatography. *Am. Lab.* 1987, **19,** 112
12. Saxena, V. and Weil, A.E. Radial flow columns: A new approach to scaling-up biopurifications. *BioChromatography* 1987, **2,** 90
13. Huang, H.S., Roy, S., Hou, K.C. and Tsao, G.T. Scaling-up of affinity chromatography by radial-flow cartridges. *Biotechnol. Prog.* 1988, **4,** 159
14. Plaigin, M., Lacoste-Bourgeacq, J.F., Mandaro, R. and Lemay, C. Purification of plasma fractions by radial flow chromatography cartridges. *Colloque INSERM.* 1989, **175,** 169
15. Rice, R.G. Approximate solutions for batch, packed tube and radial flow adsorbers—comparison with experiments. *Chem. Eng. Sci.* 1982, **37,** 83
16. Gu, T., Tsai, G.-J. and Tsao, G.T. A theoretical study of multicomponent radial flow chromatography. *Chem. Eng. Sci.* 1991, **46,** 1279
17. Gu, T., Tsai, G.-J. and Tsao, G.T. Study of multicomponent adsorption and chromatography with uneven saturation capacities. *AIChE J.* 1991, **37,** 1333
18. Fromcnt, G.F. and Bischoff, K.B. *Chemical Reactor Analysis and Design.* New York: Wiley, 1979, pp. 529–530
19. Chase, H.A. Prediction of the performance of preparative affinity chromatography. *J. Chromatogr.* 1984, **279,** 179
20. Ruthven, D.M. *Principles of adsorption and adsorption processes.* New York: Wiley, 1984, p. 106
21. Arve, B.H. and Liapis, A.I. Modeling and analysis of elution stage of biospecific adsorption in finite bath. *Biotech. Bieng.* 1988, **31,** 240